# Thermal rounding of micron-sized polymer particles in a downer reactor: direct vs indirect heating

*Juan Sebastian Gomez Bonilla and Maximilian Alexander Dechet*
Institute of Particle Technology, Friedrich-Alexander-Universitat Erlangen-Nurnberg, Erlangen, Germany
*Jochen Schmidt*
Department of Chemical and Biological Engineering, Institute of Particle Technology, Friedrich-Alexander-Universitat Erlangen-Nurnberg, Erlangen, Germany, and
*Wolfgang Peukert and Andreas Bück*
Institute of Particle Technology, Friedrich-Alexander-Universitat Erlangen-Nurnberg, Erlangen, Germany

## Abstract

**Purpose** – The purpose of this paper is to investigate the effect of different heating approaches during thermal rounding of polymer powders on powder bulk properties such as particle size, shape and flowability, as well as on the yield of process.

**Design/methodology/approach** – This study focuses on the rounding of commercial high-density polyethylene polymer particles in two different downer reactor designs using heated walls (indirect heating) and preheated carrier gas (direct heating). Powder bulk properties of the product obtained from both designs are characterized and compared.

**Findings** – Particle rounding with direct heating leads to a considerable increase in process yield and a reduction in powder agglomeration compared to the design with indirect heating. This subsequently leads to higher powder flowability. In terms of shape, indirect heating yields not only particles with higher sphericity but also entails substantial agglomeration of the rounded particles.

**Originality/value** – Shape modification via thermal rounding is the decisive step for the success of a top-down process chain for selective laser sintering powders with excellent flowability, starting with polymer particles from comminution. This report provides new information on the influence of the heating mode (direct/indirect) on the performance of the rounding process and particle properties.

**Keywords** Selective laser sintering, Polymers, Particle size, Particle shape, Crystallinity, Shape modification, Thermal rounding, Powder flowability

**Paper type** Research paper

## 1. Introduction

Additive manufacturing often referred to as "three-dimensional printing" is a set of techniques used to produce three-dimensional parts by a layer-by-layer approach without the need of forms, tools or assembly (Hague *et al.*, 2005). One such technique for production of plastic components is selective laser sintering (SLS), which allows the production of complex geometries starting from a powder bed. In SLS, powder layers are applied by means of a blade or another powder deposition system, for example, a roller coater (van der Schueren and Kruth, 1995). Once a layer of powder is applied, a laser scans the powder bed according to the geometry of the cross-section of the part to be built, defined by a computer-aided design. After solidification of the sintered layer, a new layer of powder is applied. By repeating the aforementioned steps layer-by-layer, a three-dimensional component is finally produced. Powder bed fusion processes have been successfully applied for the processing of powders of polymers, metals, ceramics and composites of these materials (Franco *et al.*, 2010; Cheng *et al.*, 2019; Zhou *et al.*, 2018; Qian and Shen, 2018; Kruth *et al.*, 2003; Savalani *et al.*, 2012).

Mechanical properties of devices produced by SLS depend strongly on the process parameters (Gibson and Shi, 1997; Pilipović *et al.*, 2016; Starr *et al.*, 2011), as well as on the intrinsic material and powder bulk properties (van Hooreweder *et al.*, 2013; Ziegelmeier *et al.*, 2015; Shi *et al.*, 2016). Desirable bulk powder properties are narrow particle size distributions with volume-averaged mean particle sizes between 50 and 100 $\mu$m and a nearly spherical shape. Powders with these properties are characterized by a high packing density and good flowability, resulting in uniform and dense layers of powders (Schmid *et al.*, 2015; Dietrich *et al.*, 2016; Sutton *et al.*, 2017). The most important process parameters affecting part properties are the laser

The current issue and full text archive of this journal is available on Emerald Insight at: **https://www.emerald.com/insight/1355-2546.htm**

Rapid Prototyping Journal
26/9 (2020) 1637–1646
 [ISSN 1355-2546]
[DOI 10.1108/RPJ-01-2020-0008]

Funded by the Deutsche Forschungsgemeinschaft (DFG, German Research Foundation) – Project-ID 61375930 – CRC 814 (Additive Manufacturing), sub-project A2. Financial support is gratefully acknowledged.

Received 14 January 2020
Revised 20 May 2020
Accepted 13 July 2020

power, scan speed, scan spacing, layer thickness, scan direction and the preheating temperature in the cases of polymers (Hofland *et al.*, 2017).

SLS powders can be produced by various processes depending on the type of material. Polymer powder materials are typically produced in one of the following four ways: direct polymerization, melt emulsification (Fanselow *et al.*, 2016), co-extrusion (Fanselow *et al.*, 2016; Kleijnen *et al.*, 2019), precipitation (Kloos *et al.*, 2018; Dechet *et al.*, 2019) or comminution (Schmidt *et al.*, 2014; Schmidt *et al.*, 2012). Comminuted powders typically exhibit irregular shaped particles with broad distributions of aspect ratios, leading to poor flowability and low packing density (Schmid, 2018; Lumay *et al.*, 2012). For that reason, comminuted particles often require shape modification to make the powder suitable for SLS. The other methods, for example, precipitation can lead to potato-shaped particles or particles with increased surface roughness (Schmid, 2018; Dechet *et al.*, 2018) and thus may also require shape modification to further increase the sphericity and decrease surface roughness.

Shape modification can be performed mechanically or thermally. In mechanical approaches, particle rounding is achieved using comminution techniques, namely, dry impact mills. These machines are provided with a rotor-stator system enclosed inside a treatment chamber (Otani *et al.*, 1994), where particles are rounded by attrition and deformation due to multiple impacts of the particles with the rotor, the walls or with other particles (Mundszinger *et al.*, 2017; Naito *et al.*, 1993). The particle shape transformation kinetics during mechanical rounding depends mainly on the rotational velocity of the rotor and the mechanical properties of the material (Otani *et al.*, 1996; Otani *et al.*, 1994). Higher velocities result in accelerated kinetics. However, velocities too high could result in the comminution of the particles (Mundszinger *et al.*, 2017). With respect to the mechanical properties, the higher the ductility of the material, the faster is the shape transformation kinetics (Otani *et al.*, 1996). Mechanical rounding can be applied to materials with moderate strength, ductile material such as metals and even to hard materials (Kondo *et al.*, 2016). Brittle materials are likely to be comminuted rather than rounded. The mechanical rounding of toner particles (Otani *et al.*, 1994), stainless steel particles (Otani *et al.*, 1996), graphite (Ohzeki *et al.*, 2005; Mundszinger *et al.*, 2017) and various pharmaceutical organic crystals (Kondo *et al.*, 2016) have been reported. In the field of additive manufacturing, mechanical rounding has been employed for the production of micro-sized polysulfone (Mys *et al.*, 2016a) and polystyrene (Mys *et al.*, 2016b) particles for SLS. In mechanical rounding, the shape transformation process is also accompanied by the reduction of particle size (Otani *et al.*, 1996). Additionally, depending of the type of device used, the production of elongated (Mys *et al.*, 2016a) or thin flake-like particles (Mundszinger *et al.*, 2017) is also observed, resulting in a broad distribution of particle shapes and a considerable modification of the particle size distribution depending on the type of raw material. Consequently, an additional classification step is necessary, to separate the unwanted fine fraction of fragments and to separate the spherical from the non-spherical particle by air classification (Mys *et al.*, 2016a; Mundszinger *et al.*, 2017). Accordingly, the yield of spherical particles is considerably decreased in mechanical rounding processes.

Thermal approaches involve the (partial) melting of particles dispersed in a gas. The molten layer induces rounding due to surface tension reducing the free surface energy by decreasing the overall surface area (Sachs *et al.*, 2017; Ji *et al.*, 2017). Thermal rounding processes can be applied to ceramic, metal and polymer systems differing mainly in the required temperature ranges and in the way and manner how the energy necessary to melt the powders is provided. In the case of metals and ceramics, thermal plasmas are used mainly (Shi *et al.*, 2016; Bissett *et al.*, 2015; Kotlyarov *et al.*, 2017; Chaturvedi *et al.*, 2014). Heat supply and transfer by flames (Jin *et al.*, 2010; Gupta *et al.*, 2018) or pulsed electron beam irradiation (Murray *et al.*, 2019) are alternative techniques. Several examples of thermal rounding of metal particles applied for additive manufacturing are reported in the literature (Chaturvedi *et al.*, 2014; Ji *et al.*, 2017; Zi *et al.*, 2017). However, reports on the thermal rounding of polymer particles are scarce. The rounding of polymer powders in a wall-heated tubular reactor in downward directed flow ("downer") was developed and has been tested for a wide range of polymer systems (Schmidt *et al.*, 2016; Dechet *et al.*, 2018; Schmidt *et al.*, 2014). Downer reactors are preferred for the rounding of particles, as a nearly plug-flow structure of the solids can be achieved and the back-mixing of particles is avoided (Lehner and Wirth, 1999; Cheng *et al.*, 2008). These features allow a more homogenous and accurate particle treatment compared with other gas-solids fluidized bed reactors, for example, a riser reactor. In the downer reactor, the material is exposed to heat provided by (indirect) wall heating. The operation of such a downer reactor has been characterized experimentally with respect to the required exposure time and temperature profile along the downer reactor length (Sachs *et al.*, 2017).

Although the quality of the obtained product was very good in terms of shape, the yield of the process was low. Depending mainly on the particle size and the triboelectric properties of the material, the yield oscillates in the range of 10–50 mass-percent related to the supplied mass of polymer. Furthermore, significant agglomeration during the rounding process took place modifying significantly the particle size distribution of the raw material and subsequently impairing the powder flowability. Agglomeration is primarily a function of the particle concentration in the reactor. To minimize the particle agglomeration the process must be operated at low concentrations. This fact limit the throughput of the process to 20 to 80 g/h.

In this contribution, we introduce direct convective heating as an alternative heating concept. We develop and compare the characteristics of both designs. In addition, the flow behavior and yield of both methods are compared, taking into account the preservation of product quality in terms of shape, size and polymer crystallinity.

## 2. Materials and methods

### 2.1 Materials

High-density polyethylene (PE-HD) (Coathylene® NB 645374, Axalta Polymer Powders, Switzerland) is used for the rounding experiments.

## 2.2 Methods

### 2.2.1 Description of the downer reactor

Rounding of the polymer particles is achieved in a stainless steel vertical tubular reactor (downer reactor) with an inner diameter of 100 mm and a total length of 1.2 m (Figure 2). The powder feed is dispersed in nitrogen (5.0, Air Liquide GmbH, Germany) by means of a flat-tray feeder (ZD 22 FB-C-2M, Three-tec GmbH, Germany) equipped with a self-made powder venturi injector operated at a pressure of 1 bar and a gas flow rate of 1 $Nm^3/h$. In the current study, the powder was fed at a rate of 200 g/h. The particles are conveyed to the reactor and are fed through a nozzle at the center of the reactor. A secondary gas flow is fed at the head of the reactor. This secondary sheath gas flow acts to reduce the interactions of the particles and the wall and to control the residence time of the particles inside the downer. The volumetric flow of the sheath gas was set at 7 $Nm^3/h$ by a mass flow controller (EL-Flow, Wagner Mess-und Regeltechnik, Germany). The sheath gas is homogeneously distributed over the downer cross-section surrounding the aerosol nozzle by means of a sintered metal plate (SIKA-R20, GKN Sinter Metals GmbH, Germany). A detailed description of the inlet section of the downer can be found elsewhere (Schmidt *et al.*, 2016; Sachs *et al.*, 2017).

Two different heating mechanisms are analyzed in this contribution. Schematic presentations of the two mechanisms (indirect and direct) are shown in Figure 1. In the indirect approach [Figure 1(a)], the reactor walls are heated by an electric oven (Thermal technology GmbH; Bayreuth, Germany) consisting of several heating sections, which can be controlled independently. In this case, the heat is transferred indirectly from the wall to the gas phase and finally to the particles by convection, conduction and radiation (Sachs *et al.*, 2017; Dechet *et al.*, 2018; Schmidt *et al.*, 2016). Indirect heating can be understood as heat transfer to a gas in a vertical pipe from pipe walls with constant temperature (set temperature of the oven). When cold sheath gas is fed centrally to the downer, a temperature profile develops, in which the lowest temperature is reached in the center and the highest temperature at the wall. The temperature difference decreases along the length of the reactor as the sheath gas heats up. This behavior was observed in the measured temperature profiles for the rounding of polybutylene terephthalate reported in (Sachs *et al.*, 2017).

In the direct heating approach [Figure 1(b)], wall heating is not used, but the sheath gas is heated using an external gas heater (GA00565, Horst GmbH, Germany). Therefore, direct heat transfer from the heated gas to the particles is achieved. Downer walls are insulated to limit the heat transfer to the environment. Direct heating corresponds to the case of heat transfer with constant heat flux to the wall. In this case, the maximum temperature is reached at the center of the downer and the minimum temperature at the wall. The temperature at the center of the reactor decreases along the length of the reactor as consequence of heat transfer through the downer walls.

In both configurations, the temperature is reduced below the melting onset of the particles, such that the particles solidify. Particles are finally separated from the process gas by a cyclone.

The aerosol flow is heated to 120°C by using a heating band (HBS, Horst GmbH, Germany) wrapped around the aerosol conveying pipe. The temperature at the inlet of the aerosol is set to 140°C and is identical for both configurations. The temperature of the wall heating and the sheath gas was set at 250°C and 140°C, respectively, to achieve a center temperature of 140°C in both designs. The mass flow of aerosol and sheath gas is set identical in both cases.

**Figure 1** Schematic representation of downer reactor with a) wall (indirect) heating and b) heated sheath gas (direct heating) for the rounding of polymer particles

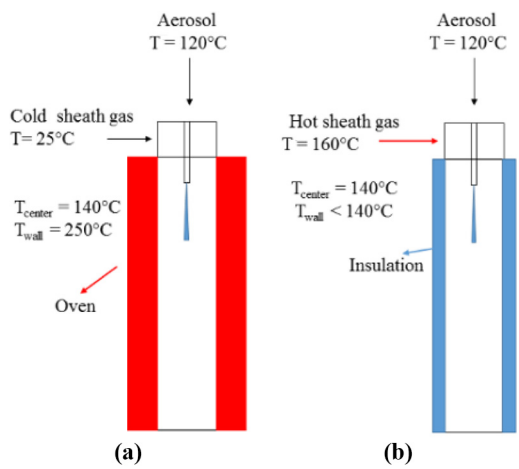


### 2.2.2 Scanning electron microscopy

Particle shape and surface morphology is characterized by scanning electron microscopy (SEM). A Gemini Ultra 55 (Carl Zeiss Microscopy GmbH, Germany) is used to take images of the particles using a SE2 detector (acceleration voltage: 1 kV).

### 2.2.3 Laser diffraction particle sizing

Particle size distribution (PSD) is determined by laser diffraction (Mastersizer 2000, Malvern Panalytical GmbH, Germany), and (Scirocco 2000, Malvern Panalytical GmbH, Germany) using the dry dispersion (Scirocco, 2000) at 50% of the vibration amplitude of the feeding tray. From the PSD, also the extent of powder agglomeration can be assessed.

### 2.2.4 Light microscopy

Light microscopy is used to determine the particle shape distribution of the raw and rounded powders. Microscope samples were prepared by spreading powder from a spatula on a glass slide. Subsequently, another glass slide is placed over the particle layer and carefully moved in circles with minimal pressure. This resulted in samples with homogenous particle distribution with few agglomerates. Images are taken by using an Axio Imager M1m light microscope (Carl Zeiss Microscopy GmbH, Germany) in transmitted light mode with a 10x objective. The motorized microscope stage allows to scan the complete slide generating an array of images. The images are transformed to binary type and are digitally analyzed for the shape factor distribution of the particles, using the extended particle analyzer of the Biovoxxel toolbox in Fiji software (Schindelin *et al.*, 2012). For the evaluation, at least 10,000 particles of each sample were analyzed. The factors selected to describe the shape of the particles were the circularity and the roundness:

$$\text{Circularity}: \quad \chi = \frac{4\pi A}{P^2} \tag{1}$$

$$\text{Roundness}: \quad r = \frac{4 \cdot A}{\pi \cdot x_{max}^2} \tag{2}$$

where $x_{max}$ is the major axis of a particle when approximated by an ellipse and $A$ and $p$ are the measured projected area and perimeter of the particle, respectively.

The circularity is a function of the particle aspect ratio and surface roughness. The dependence of the circularity on the projected area and perimeter is illustrated in Figure 3. The circularity of particles at a constant projected area can decrease by increasing the perimeter. This would be the case, for instance, for particles with an aspect ratio close to 1, but with increasing surface roughness [Figure 2(a)]. Analogously, circularity decreases at constant perimeter, if the projected area decreases. This would be the case for a particle with increasing aspect ratio [Figure 2(b)]. Spherical particles with low surface roughness would have a circularity value of 1. Roundness in turn only depends on the aspect ratio. For purely ellipsoidal particles, roundness becomes the inverse of the aspect ratio.

The analysis of both, circularity and roundness, is useful to describe the process of shape transformation, as it allows to discriminate the influence of the rounding process on the aspect ratio and surface roughness of the particles. For example, an increase of circularity after rounding, while roundness remains constant, implies a decrease of the surface roughness or rounding of the particle edges.

*2.2.5 Flowability*

A ring shear tester (RST-01.01, Dr Dietmar Schulze Schüttgutmesstechnik, Germany) was used to measure the flow behavior of the powders. The powders are filled in the tester and the measuring device was prepared according to procedures indicated in ASTM D6773 – 02. The powders were subjected to consolidation stresses of 1,450 Pa, 2,500 Pa and 5,800 Pa. The unconfined yield strength ($\sigma_c$) and the major consolidation stress ($\sigma_1$) are derived from the two Mohr stress circles according to the procedure described by Jenike (1976). The ratio $\sigma_1/\sigma_c$ is called the flow function $ff_C$. The flow function provides a measure of the flowability of the powder at a defined consolidation stress. In general, higher values of $ff_C$ represent good flowability, while small values characterize cohesive materials. A value in the range of 1–2 corresponds to very cohesive, while a value larger than 4 correspond to an easily or free flowing powder. The reported values of $ff_C$ correspond to the mean value of three independent measurements.

**Figure 2** Basic concept of shape transformation from a perfect circle when a) the perimeter increases at constant projected area and b) the area decreases at a constant perimeter

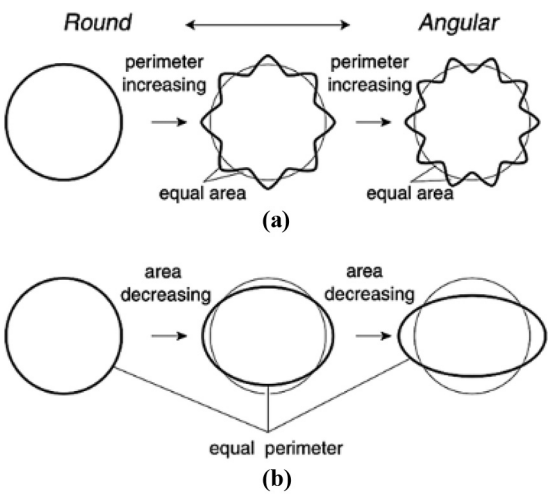


**Source:** Adapted from (Takashimizu and Iiyoshi, 2016) under Creative Commons Attribution 4.0 License

*2.2.6 Powder deposition experiment*

To qualitatively analyze the effect of the rounding process on powder deposition, a powder layer with a height of 120 $\mu$m was spread on a smooth black substrate by using a quadruple Film Applicator (Model 360, Erichsen, Germany). This experiment was performed to simulate the powder application during SLS in a machine using a doctor blade as application system. Images of the produced layers were taken and qualitatively analyzed for the coverage and homogeneity.

*2.2.7 Differential scanning calorimetry*

The effect of the rounding process on the thermal history of polymers was assessed by differential scanning calorimetry (DSC) using a DSC8000 (Perkin Elmer). For the measurements, 5 to 8 mg of sample were used. In the first heating cycle, the samples were heated at a rate of 10 K/min from 25°C to 160°C. After reaching the temperature, an isothermal step of 1 min was applied. Then, the samples were cooled to 30°C at 10 K/min. The degree of crystallinity was calculated according to the following equation (3):

$$X_c = \frac{\Delta H}{\Delta H_0} \cdot 100\% \tag{3}$$

$\Delta H$ is the heat of fusion measured by DSC and $\Delta H_0$ is the heat of fusion of the purely crystalline material. The value of $\Delta H_0$ for PE-HD is reported as 293.6 J/g (Wunderlich, 1992).

According to DSC measurements (Figure 3), melting is initiated at a temperature of 125°C and terminated at a temperature of 134°C.

**Figure 3** DSC thermogram of raw PE-HD

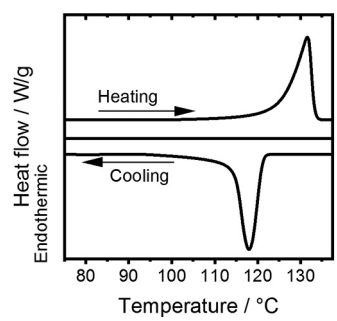

## 3. Results

### 3.1 Particle size and shape

Figure 4 shows the volume-averaged density ($q_3$) and cumulative ($Q_3$) particle size distributions of the PE-HD powder before (black continuous line) and after rounding by using the indirect (blue dotted line) and direct (red dashed line) heating approach, respectively. All distributions reveal a bimodal distribution with a first modal peak at approximately 10 $\mu$m and a second modal peak at approximately 56 $\mu$m. The mean volume-averaged particle size of the raw material is 63 $\mu$m.

The particle size of the powder increases considerable after rounding by using the indirect heating (wall-heated) approach. This is observed by considering the decrease of the intensity of the second modal peak as well as the increased amount of coarse particles with particle sizes between 100 and 350 $\mu$m. The mean volume-averaged particle size increased to 85 $\mu$m after rounding with the indirect heating approach. In comparison to the results obtained by the indirect heating approach, the increase of the particle size after rounding with the direct heating approach is considerably reduced and the original particle size distribution of the powders was altered to a lesser degree. In this case, the mean particle size distribution of the powder remains at 63 $\mu$m. The increase of the particle size after rounding is primarily the consequence of agglomeration due to collision and coalescence of partially molten polymer particles during rounding (Figure 6).

Figures 5 shows scanning electron and light microscope images of the untreated PE-HD.

The raw material is characterized by particles with a broad distribution of particle shapes, including elongated, flake-like and potato-like shaped particles. The edges of the particles are rounded and the surface of the particles is uneven.

**Figure 4** Volume-based particle size distributions of the untreated and rounded materials by using the indirect and direct heating approach

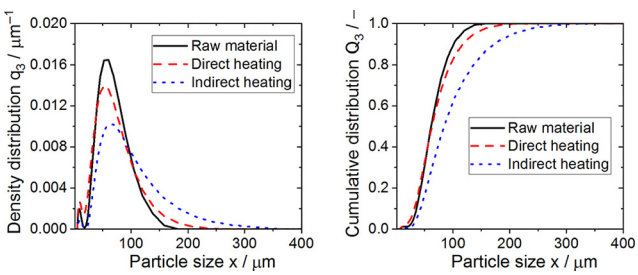


**Figure 5** Scanning electron and light microscopy images of untreated PE-HD powder

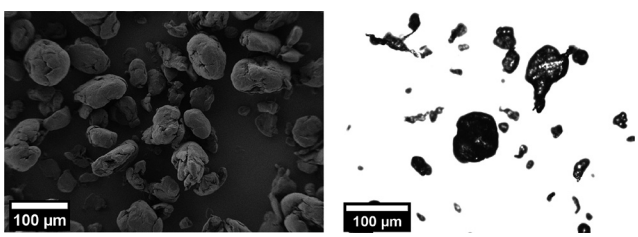


Figures 6 and 7 show the effect of the rounding process on the particle shape and surface morphology when using the indirect and direct heating approaches, respectively. In the first case (Figure 6), all particles melt completely during the process, resulting in spherical particles with smooth surfaces. Figure 6 also shows the effect of agglomeration. Spherical particles agglomerate producing larger structures at different states of coalescence. This results in some elongated structures of irregular shape with rounded edges.

The shape transformation achieved by using the direct heating approach (Figure 7) is partial. Some particles are completely rounded, while other particles are partially or not modified by the process at all. Agglomeration of particles is also observed when using the direct heating approach, however, to a much lesser extent compared to indirect heating.

The change of particle shape can be quantified considering the change of shape factor distributions. Figures 8 and 9 show

**Figure 6** Scanning electron and light microscopy images of rounded PE-HD powder using indirect heating approach

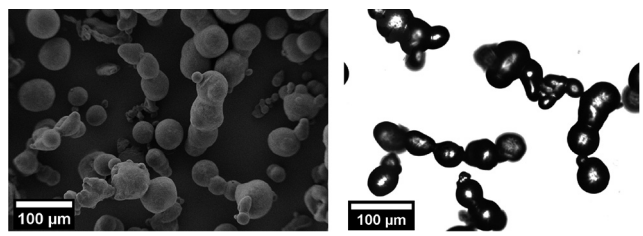


the number averaged circularity and roundness distributions of

**Figure 7** Scanning electron and light microscopy images of rounded PE-HD powder using direct heating approach

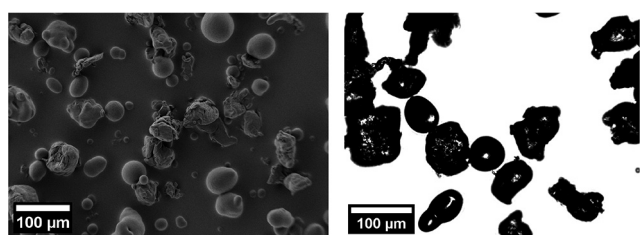


**Figure 8** Number-averaged circularity distribution of the analyzed powders

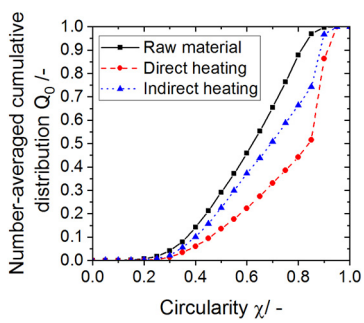

**Figure 9** Number-averaged roundness distribution of the analyzed powders

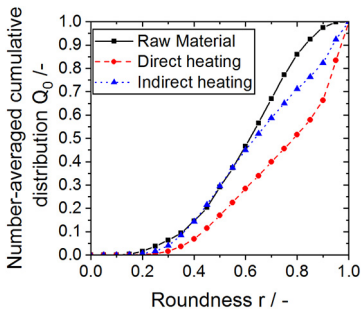


the three analyzed powders, respectively. The untreated PE-HD presents a broad distribution of circularity and roundness, which is in accordance with the variety of particles shapes described above. In both configurations, a clear shift of the circularity and roundness distributions toward higher values is observed. Higher circularity and roundness values are obtained in the direct heating approach compared to indirect heating. The inferior performance of the indirect heating is due to the formation of structures with irregular shape as consequence of the agglomeration, as discussed above. According to the particle size distribution of the powders (Figure 4), agglomeration is more pronounced in this case, leading to a decreased overall rounding effect.

In terms of yield, given as the ratio of mass of product and the mass of PE-HD fed into the reactor, the indirectly heated reactor leads to a yield of approximately $32 \pm 6\%$ (3 experiments). The remaining 68% of feed material (on average) are deposited at the reactor walls, requiring high-temperature (pyrolysis) cleaning of the apparatus after each experiment. In the directly heated configuration, a yield of $85 \pm 10\%$ was obtained. This huge improvement can be explained with the lesser risk of sticking of partially molten polymer particles at the colder reactor walls (ca. 140°C as compared to 250°C for indirect heating).

As consequence of the agglomeration during rounding (Figure 4), the rounded product would need to be classified in an additional process to obtain the desired particle size distribution for application in SLS. The "specification yield" is used here to account for the mass percentage of product between a desired (specified) particle size interval:

$$\text{spec. yield} = \left(Q_3(x_1) - Q_3(x_2)\right) * 100\% \quad (4)$$

For the analysis with respect to SLS applications, two different particle size intervals are considered: 20 to 100 $\mu$m (loose specification) and 40 to 60 $\mu$m (tight specification). The specification yields obtained for the raw and rounded materials are listed in Table 1.

**Table 1** Specification yields of the raw and rounded materials

| Specification | Specification yield/% | | |
|---|---|---|---|
| | Raw material | Direct heating | Indirect heating |
| 20 $\mu$m < x < 100 $\mu$m | 88 | 79 | 61 |
| 40 $\mu$m < x < 50 $\mu$m | 32 | 28 | 19 |

As observed in Table 1, the mass percentages of particles in intervals decrease in the rounded product compared to the raw material. The primary reason is agglomeration. This decrease is considerably higher in the indirect heating approach. The specification yields obtained for the direct heating approach are close to those of the untreated PE-HD.

The differences in the agglomeration behavior in the two setups are explained by the differences in the radial temperature distribution and by the radial particle concentration profiles in the two designs. In the downer reactor (co-current flow of gas and solids), most of the particles are concentrated in the near-wall region leading to a diluted core section (Lehner and Wirth, 1999; Zhang *et al.*, 1999; Cheng *et al.*, 2008). In the indirect heating approach, the highest temperature (significantly higher than the melting point of the material) is reached close to the reactor wall. As the melt viscosity of PE-HD decreases with increasing temperature (Vera-Sorroche *et al.*, 2014), faster and more pronounced rounding is achieved in the near-wall region. The combination of relative high particle concentration in the near wall region (compared with the reactor center), and the high temperature and the decreased melt viscosity of the partially molten particles at this region lead to an increased number of collisions between partially molten and sticky particles and thereby to increased agglomeration (Rieck *et al.*, 2018). Furthermore, the high particle concentration near the wall leads to increased particle-wall interaction, resulting in the increased adhesion of the molten particles to the wall. In total, this explains the very good shape transformation (low melt viscosity), the shift of particle size to larger sizes (agglomeration), the large amount of deposits at the reactor wall (agglomeration and adhesion) and the low overall mass yield.

In the direct heating approach, the temperature decreases toward the wall of the reactor, resulting in slower and less pronounced rounding kinetics in this region. The temperature at the near-wall region is below the melting point of the material, thus leading to the solidification of the particles. The collision between consolidated particles does not result in agglomeration as often as in the indirect heating approach. This also leads to an increased mass yield, as less particles adhere to the wall of the reactor. As a consequence, the shift toward larger particle sizes is also smaller. However, the shape transformation is less pronounced, as the temperature is only slightly above the melt temperature. This can be tuned, however, by manipulation of the inlet gas temperature.

The differences obtained between the two approaches are the result of the radial distribution of particles and temperatures in the reactors and are independent of the material and bulk properties of the raw powders. The radial distribution of the particles depends on the used configuration to mix the aerosol with the sheath gas (Zhao *et al.*, 2010; Johnston *et al.*, 1999). As the downer entrance and dimensions are exactly the same in both configurations, the solids distribution in the reactors is similar. The radial distribution of the temperature depends on the heating approach used as described above. Thus, analogous results to this investigation are expected when using other powders systems with different materials and powder bulk properties.

### 3.2 Flowability and powder deposition

Compared to the raw material, an increase in flowability (Figure 10) is observed for the material rounded by the direct heating approach. Upon rounding of the particles, the surface of the particles becomes smoother. Consequently, the number of contact points between adjacent particles is reduced and, thus, the van der Waals forces. As consequence of the rounding, the convexity of particle edges increases, reducing also the mechanical interlocking. Both factors contribute to an increased flowability. The increase is not dramatic in this case, as particle shape still differs from the optimum spherical shape. However, by additional process development and optimization of the residence time of particles above the melting temperature, further improvement of the shape distribution can be achieved. The powder rounded by the indirect heating approach (wall heating) exhibits lower flowability for the three tested consolidation stresses. This is due to the irregular elongated chain-like structures produced as consequence of agglomeration and coalescence of spherical particles during the rounding process (Figure 6). Concave necks between the partially coalesced particles can be observed. These necks increase the probability of mechanical interlocking between the particles under consolidation, increasing the resistance to flow and, thus, reducing the powder flowability.

Figure 11 shows the effect of rounding on the powder dispersion behavior. The unmodified powder leads to a non-uniform powder deposition with uncovered regions (dark regions) and regions with high particle concentration (bright regions). This would ultimately result in holes and defects in the SLS manufactured parts. After rounding, an increase of the coverage and uniformity of the dispensed layers is observed. The direct heating approach leads to more uniform and homogeneous layers compared to the indirect (wall heated) one. Thus, the rounding of particles using the direct heating approach would lead to better mechanical properties and lower porosity in comparison with powders rounded by indirect heating at the same conditions. The decreased performance of the particles treated by indirect heating is attributed to the reduced flowability and the broad particle size distribution, which leads to the application of a lesser amount of particles when using the same dispensing parameters, for example, gap width of the doctor's blade.

### 3.3 Crystallinity

The crystallinity of the PE-HD material after rounding was studied by DSC, as shown in Figure 12. The measured specific melting enthalpies are 167.93, 161.44 and 169.54 J/g for the un-treated material, the rounded product with direct heating and the rounded product with indirect heating, respectively.

The initial degree of crystallinity was determined to be 58% and remained unchanged after direct heating rounding. The crystallinity of the powder rounded in the apparatus with indirect heating decreased to 55%. These results show no drastic change in crystallinity for both configurations and a slight advantage of the direct heating design with respect to conservation of the degree of crystallinity.

**Figure 10** Results of the flowability measurements for the untreated and the two rounded PE-HD powders

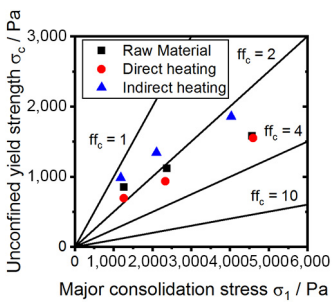


**Figure 12** Heat flow vs temperature diagram obtained from DSC measurements for rounded material with indirect and direct heating

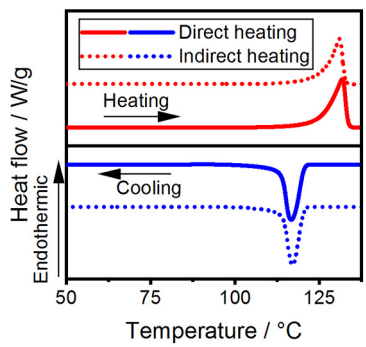


**Figure 11** Results of the application experiments of the powder with a doctor blade

**(a)** **(b)** **(c)**

**Notes:** (a) Raw material; (b) indirect heating; (c) direct heating

## 4. Conclusions and outlook

In this work, we presented an experimental study on the operation of a downer reactor for thermal rounding of polymer particles with direct convective and indirect heating of the material. We showed that direct heating is beneficial with respect to yield and flowability of the product, conserving the degree of crystallinity and better preserving also the particle size distribution of the raw material. However, shape transformation was partial and some particle remain unmodified after treatment. Conversely, indirect heating of the reactor shows better results in terms shape modification but with considerably lower product yield, flowability and crystallinity. Results were shown for PE-HD but can be transferred easily to other polymers by adjusting the temperature of the process to the system. Moreover, the presented approach for thermal rounding is scalable. Thus, it could be transferred to the plant scale and applied for rounding of SLS feedstock powders obtained by comminution and thus, improve SLS processability of these materials.

As an outlook with respect to agglomeration of the material, especially in the indirect heating configuration, an in-depth study of the micro-processes, such as partial melting, sintering of solid primary particles, coalescence of fully molten droplets, sticking to apparatus walls, fluid flow and temperature distribution is envisioned. Furthermore, the particle size of the initial material, the particle shape of the product, as well as the flow field in the reactor has to be considered to be able to design an optimal thermal rounding processes, allowing to fully control the degree of agglomeration and shape transformation.

## References

Bissett, H., van der Walt, I.J., Havenga, J.L. and Nel, J.T. (2015), "Titanium and zirconium metal powder spheroidization by thermal plasma processes", *Journal of the Southern African Institute of Mining and Metallurgy*, pp. 937-942., doi: 10.17159/2411-9717/2015/v115n10a6.

Chaturvedi, V., Ananthapadmanabhan, P.V., Chakravarthy, Y., Bhandari, S., Tiwari, N., Pragatheeswaran, A. and Das, A.K. (2014), "Thermal plasma spheroidization of aluminum oxide and characterization of the spheroidized alumina powder", *Ceramics International*, Vol. 40 No. 6, pp. 8273-8279., doi: 10.1016/j.ceramint.2014.01.026.

Cheng, Y., Wu, C., Zhu, J., Wei, F. and Jin, Y. (2008), "Downer reactor. From fundamental study to industrial application", *Powder Technology* 183(3), 364-384., doi: 10.1016/j.powtec.2008.01.022.

Cheng, Y., Xiao, Zhongxu, Zhu, Haihong, Zeng, Xiaoyan. and Wang, G. (2019), "Influence of substrate characteristics on residual stress of SLMed Inconel 718", *Rapid Prototyping Journal*, Vol. 25 No. 4, pp. 792-799., doi: 10.1108/RPJ-09-2018-0238.

Dechet, M.A., Goblirsch, A., Romeis, S., Zhao, Meng, Lanyi, F.J., Kaschta, J., et al., (2019), "Production of polyamide 11 microparticles for additive manufacturing by liquid-liquid phase separation and precipitation", *Chemical Engineering Science*, Vol. 197, pp. 11-25., doi: 10.1016/j.ces.2018.11.051.

Dechet, M.A., Gómez Bonilla, J.S., Lanzl, L., Drummer, Dietmar, Bück, A., Schmidt, Jochen. and Peukert, W. (2018), "Spherical polybutylene terephthalate (PBT)-polycarbonate (PC) blend particles by mechanical alloying and thermal rounding", *Polymers*, Vol. 10 No. 12, doi: 10.3390/polym10121373.

Dietrich, S., Wunderer, M., Huissel, A. and Zaeh, M.F. (2016), "A new approach for a flexible powder production for additive manufacturing", *Procedia Manufacturing*, Vol. 6, pp. 88-95., doi: 10.1016/j.promfg.2016.11.012.

Fanselow, S., Emamjomeh, S.E., Wirth, K.-E., Schmidt, Jochen. and Peukert, W. (2016), "Production of spherical wax and polyolefin microparticles by melt emulsification for additive manufacturing", *Chemical Engineering Science*, Vol. 141, pp. 282-292., doi: 10.1016/j.ces.2015.11.019.

Franco, A., Lanzetta, M. and Romoli, L. (2010), "Experimental analysis of selective laser sintering of polyamide powders. An energy perspective", *Journal of Cleaner Production*, Vol. 18 Nos 16/17, pp. 1722-1730., doi: 10.1016/j.jclepro.2010.07.018.

Gibson, I. and Shi, D. (1997), "Material properties and fabrication parameters in selective laser sintering process", *Rapid Prototyping Journal*, Vol. 3 No. 4, pp. 129-136., doi: 10.1108/13552549710191836.

Gupta, D., Hossain, K.M.Z., Ahmed, Ifty, Sottile, V. and Grant, D.M. (2018), "Flame-Spheroidized Phosphate-based glass particles with improved characteristics for applications in mesenchymal stem cell culture therapy and tissue engineering", *ACS Applied Materials & Interfaces*, Vol. 10 No. 31, pp. 25972-25982., doi: 10.1021/acsami.8b05267.

Hague, R., Campbell, I. and Dickens, P. (2005), "Implications on design of rapid manufacturing", *Proceedings of the Institution of Mechanical Engineers, Part C: Journal of Mechanical Engineering Science*, Vol. 217 No. 1, pp. 25-30., doi: 10.1243/095440603762554587.

Hofland, E.C., Baran, Ismet. and Wismeijer, D.A. (2017), "Correlation of process parameters with mechanical properties of laser sintered PA12 parts", *Advances in Materials Science and Engineering*, Vol. 2017 No. 5, pp. 1-11., doi: 10.1155/2017/4953173.

Jenike, A.W. (1976), "Storage and flow of solids", *Bulletin No. 123*, Vol. 53 No. 26.

Ji, L., Wang, Changzhen, Wu, Wenjie, Tan, Chao, Wang, G. and Duan, X.-M. (2017), "Spheroidization by plasma processing and characterization of stainless steel powder for 3D printing", *Metallurgical and Materials Transactions A*, Vol. 48 No. 10, pp. 4831-4841., doi: 10.1007/s11661-017-4240-5.

Jin, H., Xu, Liang. and Hou, S. (2010), "Preparation of spherical silica powder by oxygen–acetylene flame spheroidization process", *Journal of Materials Processing Technology*, Vol. 210 No. 1, pp. 81-84., doi: 10.1016/j.jmatprotec.2009.08.009.

Johnston, P.M., Zhu, J.-X., Lasa, H.I. and de; Zhang, H. (1999), "Effect of distributor designs on the flow development in downer reactor", *AIChE Journal*, Vol. 45 No. 7, pp. 1587-1592., doi: 10.1002/aic.690450720.

Kleijnen, R., Schmid, M. and Wegener, K. (2019), "Production and processing of a spherical polybutylene

terephthalate powder for laser sintering", *Applied Sciences*, Vol. 9 No. 7, p. 1308, doi: 10.3390/app9071308.

Kloos, S., Dechet, M.A., Peukert, W. and Schmidt, J. (2018), "Production of spherical semi-crystalline polycarbonate microparticles for additive manufacturing by liquid-liquid phase separation", *Powder Technology*, Vol. 335, pp. 275-284., doi: 10.1016/j.powtec.2018.05.005.

Kondo, K., Kido, Keisuke. and Niwa, T. (2016), "Spheronization mechanism of pharmaceutical material crystals processed by extremely high shearing force using a mechanical powder processor", *European Journal of Pharmaceutics and Biopharmaceutics*, Vol. 107, pp. 7-15., doi: 10.1016/j.ejpb.2016.06.021.

Kotlyarov, V.I., Beshkarev, V.T., Kartsev, V.E., Ivanov, V.V., Gasanov, A.A., Yuzhakova, E.A., *et al.*, (2017), "Production of spherical powders on the basis of group IV metals for additive manufacturing", *Inorganic Materials: Applied Research*, Vol. 8 No. 3, pp. 452-458., doi: 10.1134/S2075113317030157.

Kruth, J.P., Wang, X., Laoui, T. and Froyen, L. (2003), "Lasers and materials in selective laser sintering", *Assembly Automation*, Vol. 23 No. 4, pp. 357-371., doi: 10.1108/01445150310698652.

Lehner, P. and Wirth, K.-E. (1999), "Characterization of the flow pattern in a downer reactor", *Chemical Engineering Science*, Vol. 54 No. 22, pp. 5471-5483., doi: 10.1016/S0009-2509(99)00286-9.

Lumay, G., Boschini, F., Traina, K., Bontempi, S., Remy, J.-C., Cloots, R. and Vandewalle, N. (2012), "Measuring the flowing properties of powders and grains", *Powder Technology*, Vol. 224, pp. 19-27., doi: 10.1016/j.powtec.2012.02.015.

Mundszinger, M., Farsi, Sarvenaz, Rapp, M., Golla-Schindler, Ute, Kaiser, Ute. and Wachtler, M. (2017), "Morphology and texture of spheroidized natural and synthetic graphites", *Carbon*, Vol. 111, pp. 764-773., doi: 10.1016/j.carbon.2016.10.060.

Murray, J.W., Simonelli, M., Speidel, A., Grant, D.M. and Clare, A.T. (2019), "Spheroidisation of metal powder by pulsed electron beam irradiation", *Powder Technology*, Vol. 350, pp. 100-106, doi: 10.1016/j.powtec.2019.03.041.

Mys, N., van de Sande, R., Verberckmoes, A. and Cardon, L. (2016a), "Processing of polysulfone to free flowing powder by mechanical milling and spray drying techniques for use in selective laser sintering", *Polymers*, Vol. 8 No. 4, doi: 10.3390/polym8040150.

Mys, N., Verberckmoes, A. and Cardon, L. (2016b), "Processing of syndiotactic polystyrene to microspheres for part manufacturing through selective laser sintering", *Polymers*, Vol. 8 No. 11, doi: 10.3390/polym8110383.

Naito, M., Kondo, Akira. and Yokoyama, T. (1993), "Applications of comminution techniques for the surface modification of powder materials", *ISIJ International*, Vol. 33 No. 9, pp. 915-924., doi: 10.2355/isijinternational.33.915.

Ohzeki, K., Saito, Y., Golman, B. and Shinohara, K. (2005), "Shape modification of graphite particles by rotational impact blending", *Carbon*, Vol. 43 No. 8, pp. 1673-1679., doi: 10.1016/j.carbon.2005.02.007.

Otani, Masaru, Minoshima, Hironori, Ura, Tetsuya. and Shinohara, K. (1996), "Mechanism of particle shape modification by dry impact blending", *Advanced Powder Technology*, Vol. 7 No. 4, pp. 291-303., doi: 10.1016/S0921-8831(08)60488-4.

Otani, Masaru, Uchiyama, Tomoyuki, Minosima, Hironori, Shinohara, Kunio, Takasashiki, Kunihito. and Nara, N. (1994), "Factors on particle shape control by dry impact blending method", *Journal of Society of Materials Engineering for Resources of Japan*, Vol. 7 No. 2, pp. 35-45., doi: 10.5188/jsmerj.7.2_35.

Pilipović, A., Valentan, Bogdan. and Šercer, M. (2016), "Influence of SLS processing parameters according to the new mathematical model on flexural properties", *Rapid Prototyping Journal*, Vol. 22 No. 2, pp. 258-268., doi: 10.1108/RPJ-08-2014-0092.

Qian, B. and Shen, Z. (2018), "Laser sintering of ceramics", *Journal of Asian Ceramic Societies*, Vol. 1 No. 4, pp. 315-321., doi: 10.1016/j.jascer.2013.08.004.

Rieck, C., Schmidt, M., Bück, A. and Tsotsas, E. (2018), "Monte Carlo modeling of binder-less spray agglomeration in fluidized beds", *AIChE Journal*, Vol. 64 No. 10, pp. 3582-3594., doi: 10.1002/aic.16349.

Sachs, M., Friedle, M., Schmidt, Jochen, Peukert, W. and Wirth, K.-E. (2017), "Characterization of a downer reactor for particle rounding", *Powder Technology*, Vol. 316, pp. 357-366., doi: 10.1016/j.powtec.2017.01.006.

Savalani, M.M., Hao, L., Dickens, P.M., Zhang, Y., Tanner, K.E. and Harris, R.A. (2012), "The effects and interactions of fabrication parameters on the properties of selective laser sintered hydroxyapatite polyamide composite biomaterials", *Rapid Prototyping Journal*, Vol. 18 No. 1, pp. 16-27., doi: 10.1108/13552541211193467.

Schindelin, J., Arganda-Carreras, I., Frise, Erwin, Kaynig, V., Longair, Mark, Pietzsch, T., *et al.*, (2012), "Fiji: an open-source platform for biological-image analysis", *Nature Methods*, Vol. 9 No. 7, pp. 676-682., doi: 10.1038/nmeth.2019.

Schmid, M. (2018), "Laser sintering with plastics", *Technology, Processes, and Materials*, 1st ed., Hanser Publishers; Hanser Publications, Cincinnati, Munich.

Schmid, M., Amado, A. and Wegener, K. (2015), "Polymer powders for selective laser sintering (SLS)", *PROCEEDINGS OF PPS-30: The 30th International Conference of the Polymer Processing Society – Conference Papers, AIP Publishing LLC (AIP Conference Proceedings), Cleveland, OH.*

Schmidt, J., Plata, M., Tröger, Sulay. and Peukert, W. (2012), "Production of polymer particles below 5$\mu$m by wet grinding", *Powder Technology*, Vol. 228, pp. 84-90., doi: 10.1016/j.powtec.2012.04.064.

Schmidt, J., Sachs, M., Blümel, C., Winzer, B., Toni, Franziska, Wirth, K.-E. and Peukert, W. (2014), "A novel process route for the production of spherical LBM polymer powders with small size and good flowability", *Powder Technology*, Vol. 261, pp. 78-86., doi: 10.1016/j.powtec.2014.04.003.

Schmidt, J., Sachs, M., Fanselow, S., Zhao, Meng, Romeis, S., Drummer, D. (2016), "Optimized polybutylene terephthalate powders for selective laser beam melting", *Chemical Engineering Science*, Vol. 156, pp. 1-10., doi: 10.1016/j.ces.2016.09.009.

Shi, Y., Li, Z., Sun, H., Huang, S. and Zeng, F. (2016), "Effect of the properties of the polymer materials on the quality of selective laser sintering parts", *Proceedings of the Institution of Mechanical Engineers, Part L: Journal of Materials: Design and Applications*, Vol. 218 No. 3, pp. 247-252., doi: 10.1177/146442070421800308.

Starr, T.L., Gornet, T.J. and Usher, J.S. (2011), "The effect of process conditions on mechanical properties of laser-sintered nylon", *Rapid Prototyping Journal*, Vol. 17 No. 6, pp. 418-423., doi: 10.1108/13552541111184143.

Sutton, A.T., Kriewall, C.S., Leu, M.C. and Newkirk, J.W. (2017), "Powder characterisation techniques and effects of powder characteristics on part properties in powder-bed fusion processes", *Virtual and Physical Prototyping*, Vol. 12 No. 1, pp. 3-29., doi: 10.1080/17452759.2016.1250605.

Takashimizu, Y. and Iiyoshi, M. (2016), "New parameter of roundness R. Circularity corrected by aspect ratio", *Progress in Earth and Planetary Science*, Vol. 3 No. 1, p. 36, doi: 10.1186/s40645-015-0078-x.

van der Schueren, B. and Kruth, J.P. (1995), "Powder deposition in selective metal powder sintering", *Rapid Prototyping Journal*, Vol. 1 No. 3, pp. 23-31., doi: 10.1108/13552549510094241.

van Hooreweder, Brecht, Moens, David, Boonen, R., Kruth, J.-P. and Sas, P. (2013), "On the difference in material structure and fatigue properties of nylon specimens produced by injection molding and selective laser sintering", *Polymer Testing*, Vol. 32 No. 5, pp. 972-981, doi: 10.1016/j.polymertesting.2013.04.014.

Vera-Sorroche, J., Kelly, A.L., Brown, E.C., Gough, T., Abeykoon, Chamil, Coates, P.D. (2014), "The effect of melt viscosity on thermal efficiency for single screw extrusion of HDPE", *Chemical Engineering Research and Design*, Vol. 92 No. 11, pp. 2404-2412., doi: 10.1016/j.cherd.2013.12.025.

Wunderlich, B. (1992), *Thermal Analysis. [Nachdr.]*, Acad. Press, Boston.

Zhang, H., Zhu, J.-X. and Bergougnou, M.A. (1999), "Hydrodynamics in downflow fluidized beds (1). Solids concentration profiles and pressure gradient distributions", *Chemical Engineering Science*, Vol. 54 No. 22, pp. 5461-5470, doi: 10.1016/S0009-2509(99)00284-5.

Zhao, Y., Ding, Y., Wu, C. and Cheng, Y. (2010), "Numerical simulation of hydrodynamics in downers using a CFD–DEM coupled approach", *Powder Technology* 199(1), 2-12, doi: 10.1016/j.powtec.2009.04.014.

Zhou, B., Zhou, Jun, Li, Hongxin. and Lin, F. (2018), "A study of the microstructures and mechanical properties of $Ti_6Al_4V$ fabricated by SLM under vacuum", *Materials Science and Engineering: A*, Vol. 724, pp. 1-10., doi: 10.1016/j.msea.2018.03.021.

Zi, X., Chen, Chao, Wang, Xiaojun, Wang, Pengwei, Zhang, Xiaoyong. and Zhou, K. (2017), "Spheroidisation of tungsten powder by radio frequency plasma for selective laser melting", *Materials Science and Technology*, Vol. 34 No. 6, pp. 735-742., doi: 10.1080/02670836.2017.1410955.

Ziegelmeier, S., Christou, Panagiotis, Wöllecke, Frank, Tuck, Christopher, Goodridge, Ruth, Hague, R. (2015), "An experimental study into the effects of bulk and flow behaviour of laser sintering polymer powders on resulting part properties", *Journal of Materials Processing Technology*, Vol. 215, pp. 239-250., doi: 10.1016/j.jmatprotec.2014.07.029.

## Corresponding author

**Andreas Bück** can be contacted at: andreas.bueck@fau.de